D1-Asp170 Is Structurally Coupled to the Oxygen Evolving Complex in Photosystem II As Revealed by Light-Induced Fourier Transform Infrared Difference Spectroscopy†

Hsiu-An Chu,‡ Richard J. Debus,*,§ and Gerald T. Babcock*,‡

Department of Chemistry, Michigan State University, East Lansing, Michigan 48824, and Department of Biochemistry, University of California at Riverside, Riverside, California 92521-0129

Received October 2, 2000; Revised Manuscript Received December 5, 2000

ABSTRACT: We report both mid-frequency (1800−1200 cm^{-1}) and low-frequency (670−350 cm^{-1}) S_2/S_1 FTIR difference spectra of photosystem II (PSII) particles isolated from wild-type* and D1-D170H mutant cells of the cyanobacterium *Synechocystis* sp. PCC 6803. Both mid- and low-frequency S_2/S_1 spectra of the *Synechocystis* wild-type* PSII particles closely resemble those from spinach PSII samples, which confirms an earlier result by Noguchi and co-workers [Noguchi, T., Inoue, Y., and Tang, X.-S. (1997) *Biochemistry 36*, 14705−14711] and indicates that the coordination environment of the oxygen evolving complex (OEC) in *Synechocystis* is very similar to that in spinach. We also found that there is no appreciable difference between the mid-frequency S_2/S_1 spectra of wild-type* and of D1-D170H mutant PSII particles, from which we conclude that D1-Asp170 does not undergo a significant structural change during the S_1 to S_2 transition. This result also suggests that, if D1-Asp170 ligates Mn, it does not ligate the Mn ion that is oxidized during the S_1 to S_2 state transition. Finally, we found that a mode at 606 cm^{-1} in the low-frequency wild-type* S_2/S_1 spectrum shifts to 612 cm^{-1} in the D1-D170H mutant spectrum. Because this 606 cm^{-1} mode has been previously assigned to an Mn−O−Mn cluster mode of the OEC [Chu, H.-A., Sackett, H., and Babcock, G. T. (2000) *Biochemistry 39*, 14371−14376], we conclude that D1-Asp170 is structurally coupled to the Mn−O−Mn cluster structure that gives rise to this band. Our results suggest that D1-Asp170 either directly ligates Mn or Ca^{2+} or participates in a hydrogen bond to the Mn_4Ca^{2+} cluster. Our results demonstrate that combining FTIR difference spectroscopy with site-directed mutagenesis has the potential to provide insights into structural changes in Mn and Ca^{2+} coordination environments in the different S states of the OEC.

Photosynthetic water oxidation take places in photosystem II (PSII)[1] near the lumenal surface of the thylakoid membrane in plants, green algae, and cyanobacteria. The oxygen evolving complex (OEC) in PSII is composed of a tetranuclear manganese−oxo cluster and a nearby, redox active tyrosine residue, Yz [for review, see (*1*−*5*)]. Both Ca^{2+} and Cl^- ions are required for activity, but their exact structural and functional role is still not clear (*1*−*5*). The water oxidation reaction goes through a light-driven cycle of five "S_n-state" intermediates ($n = 0-4$, n representing the storage of oxidizing equivalents in the OEC) (*6*, *7*). The S_1 state predominates in dark-adapted samples. When the S_4 state is reached, O_2 is released, and the S_0 state is regenerated.

The OEC is believed to be coordinated primarily by oxygen ligands (oxo, hydroxo, aqua, and carboxylato ligands) (*5*, *8*). Coordination by at least one histidine ligand has also been shown by ESEEM and FTIR studies (*9*, *10*). Several lines of evidence suggest that the D1 polypeptide contributes most or all of the amino acid residues that coordinate the Mn and Ca^{2+} ions in PSII [for recent review, see (*2*, *11*, *12*]. Site-directed mutagenesis studies have identified D1-Asp170, D1-His190, D1-His332, D1-Glu333, D1-His337, D1-Asp342, and the C-terminus of Ala344 in D1 as potential ligands to the Mn cluster (*2*, *11*, *12*). Several carboxylate stretching modes and one histidine mode have been identified in the mid-frequency (1000−2000 cm^{-1}) S_2/S_1 FTIR difference spectrum of intact PSII samples (*10*, *13*, *14*). These carboxylate and histidine modes have been proposed to originate from carboxylate and histidine ligands of the OEC that undergo structural changes during the S_1 to S_2 transition (*10*, *13*, *14*). The exact amino acid origins of these carboxylate and histidine modes are yet to be determined. Low-frequency S_2/S_1 spectra (1000−350 cm^{-1}) have been recently reported (*15*, *16*), and one mode at 606 cm^{-1} has been

† This work was supported by the National Institutes of Health (GM43496 to R.J.D. and GM 37300 to G.T.B.) and by the USDA Competitive Research Grants Office (to G.T.B.).

‡ Michigan State University.

§ University of California at Riverside.

[1] Abbreviations: EPR, electron paramagnetic resonance; ESEEM, electron spin−echo envelope modulation; EXAFS, extended X-ray absorption fine structure; FTIR, Fourier transform infrared spectroscopy; MES, 2-(*N*-morpholino)ethanesulfonic acid; OEC, oxygen evolving complex; OTG, octyl-β-D-thioglucopyranoside; PSII, photosystem II; TES, *N*-tris(hydroxymethyl)methyl-2-aminoethanesulfonic acid; wild-type*, control strain of *Synechocystis* sp. PCC 6803 constructed in an identical fashion as the D1-D170H mutant, but containing the wild-type *psb*A-2 gene; Yz, tyrosine 161 of the D1 polypeptide.

10.1021/bi0022994 CCC: $20.00
Published on Web 01/19/2001

assigned to a Mn−O−Mn cluster mode of the OEC (*17*, *18*). The low-frequency FTIR technique has the great potential to provide direct insights into structural changes in Mn and Ca^{2+} coordination environments in the different S states of the OEC in PSII.

Several mutagenesis and spectroscopic studies have suggested that D1-Asp170 is most likely a ligand to the Mn cluster. Mutants constructed at this residue impair the function or assembly of the Mn cluster (*19*−*24*). In addition, a recent EPR study concluded that this residue directly ligates the first Mn(II) ion that is photooxidized during photoassembly of the PSII Mn cluster (*25*). However, a mutagenesis study shows that the *Synechocystis* D1-D170V mutant is weakly photoautotrophic and that the D1-D170I and D1-D170L mutants, while not photoautotrophic, are capable of O_2 evolution (*24*). Furthermore, D1-D170H PSII particles exhibit normal multiline EPR signals in the both the S_1 (K. A. Campbell, R. D. Britt, and R. J. Debus, unpublished observations) and S_2 states (X.-S. Tang and B. A. Diner, personal communications; K. A. Campbell, R. D. Britt, and R. J. Debus, unpublished observations). Therefore, a definitive conclusion as to whether D1-Asp170 ligates the *assembled* Mn cluster requires further study.

To this end, we present both mid-frequency and low-frequency FTIR difference spectra obtained with PSII particles isolated from wild-type* and D1-D170H mutant cells of the cyanobacterium *Synechocystis* sp. PCC 6803. The D1-D170H mutant is of particular interest because the *assembled* Mn clusters in this mutant evolve O_2, support photoautotrophic growth, and exhibit normal S_1 and S_2 state multiline EPR signals, whereas the first photoactivation intermediate in this mutant [a Mn(III) ion] shows an altered parallel mode EPR signal (*25*).

MATERIALS AND METHODS

Construction of Site-Directed Mutants. The D1-D170H mutation was constructed in the *psbA-2* gene of the cyanobacterium *Synechocystis* sp. PCC 6803 (*22*). The plasmid bearing this mutation was transformed into a host strain of *Synechocystis* that lacks all three *psbA* genes (*26*) and contains a hexahistidine-tag (His-tag) fused to the C-terminus of CP47 (*27*). Single colonies were selected for ability to grow on solid media containing 5 μg/mL kanamycin monosulfate (*26*). The control wild-type* strain was constructed in an identical fashion as the D1-D170H mutant except that the transforming plasmid carried no site-directed mutation. The designation "wild-type*" differentiates this strain from the native wild-type strain that contains all three *psbA* genes and is sensitive to antibiotics.

Propagation of Cultures. Wild-type* and D1-D170H cells were maintained on solid BG-11 media (*28*) containing 5 mM TES−NaOH (pH 8.0), 0.3% (w/v) sodium thiosulfate, 5 mM glucose, 10 μM DCMU, and 5 μg/mL kanamycin monosulfate, as described previously (*26*). The DCMU, kanamycin monosulfate, and sodium thiosulfate were omitted from liquid cultures. For isolation of PSII particles, cells were grown in modified 250 mL Erlenmeyer flasks until they reached an optical density of 0.9−1.2 at 730 nm. Cells were then transferred to two 20 L carboys, each containing 15 L of growth medium, and grown as described previously (*29*) until their optical densities reached 0.9−1.2 at 730 nm (typically 4 days for wild-type* and 5 days for D1-D170H cells). Optical densities were measured with a CARY 219 spectrophotometer.

Isolation of Synechocystis PSII Particles. Thylakoid membranes were isolated (50−100 mg of Chl from 30 L of cells) and extracted with *n*-dodecyl β-D-maltoside (Anatrace Inc., Maumee, OH) as described by Tang and Diner (*30*) with minor modification (*29*). The soluble *n*-dodecyl β-D-maltoside extract was mixed with 40 mL of Ni−NTA superflow affinity resin (Qiagen Inc., Valencia, CA) that had been equilibrated with sample buffer [25% (v/v) glycerol, 50 mM MES−NaOH (pH 6.0), 20 mM $CaCl_2$, 5 mM $MgCl_2$, 0.03% (w/v) *n*-dodecyl β-D-maltoside] in a 5 cm diameter chromatography column. The column was stoppered and placed on a nutatory platform for 30 min of gentle agitation in darkness. The column was then allowed to pack by gravity, and the resin was washed with 10−20 volumes of sample buffer to remove PSI and other contaminants. Purified PSII particles were eluted in 7−10 column volumes with sample buffer containing 25 mM histidine. The eluent was brought to 1 mM EDTA, concentrated by ultrafiltration (Amicon models 2000 and 8400 fitted with YM-100 membranes) to a volume of 5−10 mL, brought to 6 mM EDTA, passed through a G-25 column to remove histidine, EDTA, and EDTA-complexed metal ions, then concentrated to 1−2 mg of Chl/mL (Amicon models 8050 and 8010 fitted with YM-100 membranes), frozen in liquid N_2, and stored at −80 °C. For FTIR experiments, PSII particles were transferred into sucrose buffer [0.4 M sucrose, 50 mM MES−NaOH (pH 6.0), 20 mM $CaCl_2$, 5 mM $MgCl_2$, 0.03% (w/v) *n*-dodecyl β-D-maltoside] by passage through a G-25 column, then concentrated to 4−7 mg of Chl/mL by ultrafiltration (Amicon models 8050 and 8010 fitted with YM-100 membranes) followed by Centricon-100 concentrators (Millipore Corp., Bedford, MA), frozen in liquid N_2, and stored at −80 °C until use. The O_2 evolution activity of the wild-type* and D1-D170H PSII particles was 2.6−4.0 and 1.7−2.2 mmol of O_2 (mg of Chl)$^{-1}$ h^{-1}, respectively. Chlorophyll concentrations and light-saturated rates of oxygen evolution were measured as described previously (*24*, *29*).

Isolation of the Spinach PSII Reaction Center Cores. Spinach OTG PSII reaction center cores (RCCs), retaining the three extrinsic polypeptides, were prepared as described in (*31*). Typical oxygen evolution rates were about 1.4 mmol of O_2 (mg of Chl)$^{-1}$ h^{-1} (*15*).

Sample Conditions for FTIR Measurement. Before FTIR measurements, *Synechocystis* PSII particles were diluted with 2 volumes of double distilled water and then reconcentrated to a final concentration of 4−7 mg of Chl/mL by using Microcon-100 microconcentrators (Millipore Corp.). Sample conditions for spinach PSII RCCs were the same as described in (*10*). An aliquot of PSII (about 30−35 μg of chlorophyll) was deposited onto 25 mm diameter AgBr IR windows (Wilmad). Then 2 μL of 10 mM fresh ferricyanide stock was added as the electron acceptor. The samples were then dried under a stream of dry nitrogen gas at 4 °C. The sample concentration and thickness were adjusted so that the absolute absorbance of the amide I band of the sample was less than 1.0 absorbance unit.

Experimental Conditions for FTIR Measurement. Mid-frequency FTIR experiments were performed on a Bruker EQUINOX 55 spectrometer with a KBr beam splitter and

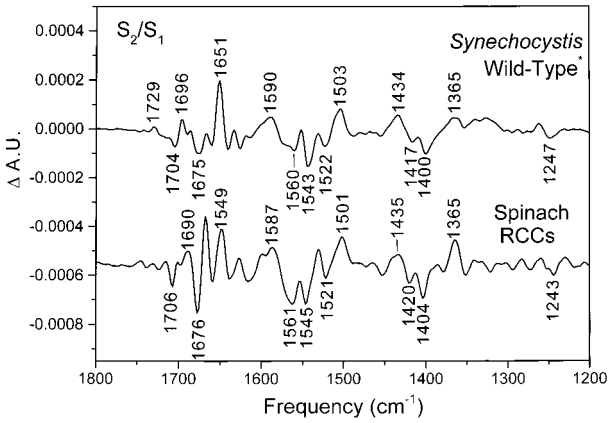

FIGURE 1: Comparison of the mid-frequency (1800−1200 cm^{-1}) S_2/S_1 FTIR difference spectra of *Synechocystis* wild-type* PSII particles (top spectrum, 1326 scans) and spinach PSII RCCs (bottom spectrum, 1326 scans) at 250 K, in the presence of ferricyanide. Both spectra were collected at 4 cm^{-1} resolution.

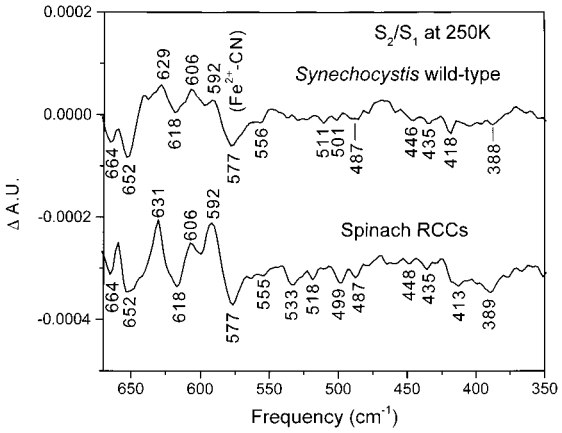

FIGURE 2: Comparison of the low-frequency (670−350 cm^{-1}) S_2/S_1 FTIR difference spectra of *Synechocystis* wild-type* PSII particles (top spectrum, 1500 scans) and spinach PSII RCCs (bottom spectrum, 450 scans) at 250 K, in the presence of ferricyanide. Both spectra were collected at 4 cm^{-1} resolution.

midrange or wide-band MCT detectors. Samples were cooled to 250 K by using a home-built liquid nitrogen cryostat (*16*). The sample temperature was regulated to ±0.01 K with a temperature controller (LakeShore 340). Low-frequency FTIR experiments were performed on a Bomen MB101 spectrometer with a CsI beam splitter and a liquid-He-cooled Si bolometer previously described (*16*). The sample temperature was regulated to ±0.1 K with a temperature controller (LakeShore 321). Samples were illuminated by a single flash from a frequency-doubled Nd:YAG laser (Quanta-Ray GCR-11) [532 nm, ∼7 ns, ∼30 mJ/(pulse·cm^2)]. S_2/S_1 FTIR difference spectra were calculated by subtracting the spectrum obtained before illumination from that after illumination.

RESULTS

A comparison of S_2/S_1 FTIR difference spectra of wild-type* PSII preparations from *Synechocystis* sp. PCC 6803 with those of spinach reaction center core (RCC) preparations in the mid-frequency and low-frequency regions is shown in Figures 1 and 2, respectively. We found that the mid-frequency region (1800−1200 cm^{-1}) of the S_2/S_1 spectrum (Figure 1) of *Synechocystis* wild-type* PSII preparations

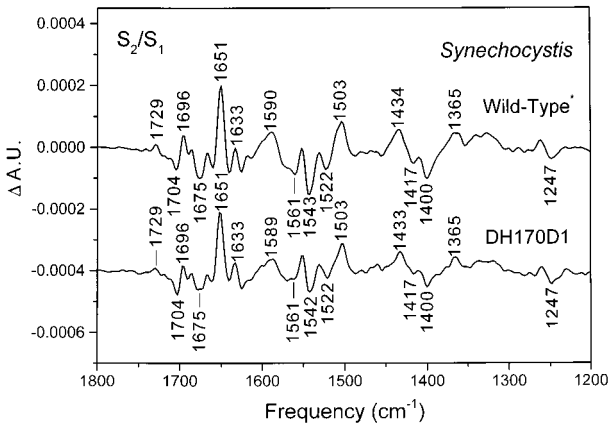

FIGURE 3: Comparison of the mid-frequency (1800−1200 cm^{-1}) S_2/S_1 FTIR difference spectra of *Synechocystis* wild-type* (top spectrum, 1326 scans) and D1-D170H mutant (bottom spectrum, 1326 scans) PSII particles. The D1-D170H mutant spectrum is normalized by multiplying by a factor of 1.5. Both spectra were collected at 4 cm^{-1} resolution.

closely resembles that of spinach RCC preparations, except there are some spectral differences in the amide I region (around 1650 cm^{-1}). Our observations reproduce closely the results from a recent FTIR study by Noguchi and co-workers (*34*). The authors of this earlier study suggest that the spectral differences in the amide I region between *Synechocystis* and spinach may be due to species variability and/or to differences in sample preparations and conditions (*34*). Both our observations and those reported earlier (*35*) show that the S_2/S_1 spectrum of *Synechocystis* wild-type* PSII particles containing a His-tag on CP47 reproduces closely the spectral features of *Synechocystis* wild-type PSII particles lacking a His-tag, even in the amide I region. The His-tag permits PSII particles to be isolated by Ni^{2+}-affinity chromatography and at low ionic strength (*32, 33*). Isolation at low ionic strength avoids the dissociation of the extrinsic *psb*U and *psb*V proteins (the ∼12 kDa protein and cytochrome *c*-550, respectively) (*32, 33*) and the accompanying loss of the Mn cluster that is often associated with previous isolation methods employing DEAE chromatography [e.g., (*30*)]. Our results show that the presence of the His-tag does not perturb the structure and protein environment of the OEC in PSII particles from *Synechocystis* sp. PCC 6803.

The low-frequency region (670−350 cm^{-1}) of the S_2/S_1 FTIR difference spectrum (Figure 2) of *Synechocystis* wild-type* PSII preparations also closely resembles that of spinach RCC preparations. For example, positive bands at ∼630 and 606 cm^{-1} and negative bands at 664, 652, 618, and 577 cm^{-1} are present in both *Synechocystis* and spinach S_2/S_1 spectra. There are some slight differences between these two spectra (e.g., at ∼500 cm^{-1}) that might originate from low-frequency amide modes, as we observed in the mid-frequency amide I regions.

A comparison of the mid-frequency and low-frequency S_2/S_1 FTIR difference spectra of *Synechocystis* wild-type* PSII preparations with those of D1-D170H preparations is shown in Figures 3 and 4, respectively. In the mid-frequency region (1800−1200 cm^{-1}) of the S_2/S_1 spectra (Figure 3), we found that the D170H spectrum shows no appreciable change compared to the wild-type* spectrum. For example, bands typical of symmetric (1365, 1400, 1417, and 1434

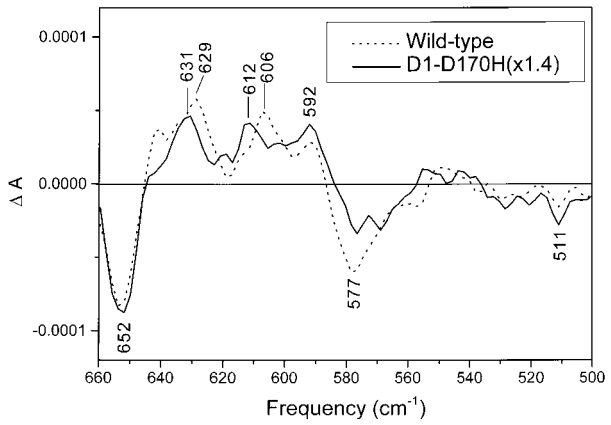

FIGURE 4: Comparison of the low-frequency (660−500 cm^{-1}) S_2/S_1 FTIR difference spectra of *Synechocystis* wild-type* (dashed line, 1500 scans) and D1-D170H mutant (bottom spectrum, 1500 scans) PSII particles. The D1-D170H mutant spectrum is normalized by multiplying by a factor of 1.4. Both spectra were collected at 4 cm^{-1} resolution.

cm^{-1}) and asymmetric CO stretching modes of carboxylate and of the amide II modes (1503, 1522, 1543, 1561, and 1590 cm^{-1}) are present practically in the same positions in both wild-type* and D1-D170H spectra. In contrast, in the low-frequency region (670−500 cm^{-1}) (Figure 4), we found one band at 606 cm^{-1} in the wild-type* spectrum that shifts to 612 cm^{-1} in the D1-D170H spectrum. This 606 cm^{-1} mode in the low-frequency S_2/S_1 spectrum has been previously assigned to an Mn−O−Mn cluster mode of the OEC (*17*, *18*). Therefore, our results suggest that the D1-Asp170 residue is coupled to the Mn−O−M cluster in the OEC that gives rise to this band.

DISCUSSION

In this study, we found that both the mid-frequency and low-frequency regions of S_2/S_1 FTIR spectra of *Synechocystis* and spinach PSII samples show strong similarities. Therefore, our results provide solid evidence that the coordination environment and structure of the OEC in these two species (a cyanobacterium and a higher plant) are very similar. The same conclusion was made in previous EPR and Mn X-ray absorption studies (*36*, *37*).

We also found that the S_2/S_1 spectrum of PSII particles isolated from D170H cells shows no appreciable changes in the mid-frequency S_2/S_1 spectrum (Figure 3). Based on this observation, we conclude that D1-Asp170 does not undergo a significant structural change during the S_1 to S_2 transition and, therefore, is not the origin of the carboxylate CO stretching modes observed in the S_2/S_1 difference spectrum (refs *13*, *14*, and Figures 1 and 3). Our results conflict with a previous FTIR study whose authors concluded that the carboxylate stretching modes of D1-Asp170 are changed during the S_1 to S_2 transition (*38*). However, the wild-type spectrum reported in (*38*) is unlike that reported elsewhere (refs *13*, *15*, *39*, *40* and Figure 1). In particular, the positive mode at 1365 cm^{-1} and the negative mode at 1400 cm^{-1}, clear markers in the S_2/S_1 spectrum (refs *13*, *15*, *39*, *40* and Figure 1), are absent in the wild-type spectrum reported in (*38*). A recent FTIR study (*41*) shows that the wild-type spectrum reported in (*38*) is probably distorted by heating artifacts associated with prolonged sample illumination.

Our low-frequency S_2/S_1 FTIR data obtained with D1-D170H PSII particles suggest that D1-Asp170 is coupled to the Mn−O−Mn structure that gives rise to the oxygen isotope-sensitive 606 cm^{-1} mode. There are several means by which this coupling can occur. The first is that D1-Asp170 directly ligates the assembled Mn cluster as proposed previously (*19*−*23*). If the Mn−O−Mn mode at 606 cm^{-1} arises from a $[Mn(\mu\text{-}O)]_2$ structure, additional insight is available from model compound work. In Mn models with the $[Mn(\mu\text{-}O)]_2$ structure, the $[Mn(\mu\text{-}O)]_2$ core mode occurs at higher frequency (about 700−650 cm^{-1}) in compounds with predominantly nitrogen ligands and shifts to lower frequency in compounds with predominantly oxygen ligands (about 650−595 cm^{-1}) (ref *17*; N. A. Law, and G. T. Babcock, unpublished results; J. S. Vrettos and G. W. Brudvig, personal communication). If the carboxylate ligand of D1-Asp170 is replaced by the imidazole moiety of histidine in the D1-D170H mutant, then the 6 cm^{-1} upshift of the 606 cm^{-1} mode in the D1-D170H spectrum is consistent with this trend. Furthermore, our mid-frequency FTIR results show that D1-Asp170 does not undergo significant structural change during the S_1 to S_2 transition. Therefore, if D1-Asp170 directly ligates Mn, it must not ligate the Mn ion that is oxidized during the S_1 to S_2 state transition. This argument might account for the observations that D1-D170H PSII particles exhibit normal multiline EPR spectra in both the S_1 state (K. A. Campbell, R. D. Britt, and R. J. Debus, unpublished observations) and the S_2 state (X.-S. Tang and B. A. Diner, personal communication; K. A. Campbell, R. D. Britt, and R. J. Debus, unpublished observations). That the first photoactivation intermediate of D1-D170H PSII particles exhibits an altered form of the Mn(III) parallel mode EPR spectrum (*25*) then suggests that this Mn ion, the first assembled into the Mn cluster, is not oxidized during the $S_1 \rightarrow S_2$ transition. The second possibility is that D1-Asp170 ligates Ca in the OEC. This proposal is supported by the observation that this 606 cm^{-1} mode upshifts to 618 cm^{-1} when Ca^{2+} is replaced by Sr^{2+} (*17*, *18*). However, there is no other direct experimental evidence to support this proposal. The third possibility is that D1-Asp170 participates in a hydrogen bond to the Mn_4Ca cluster. A perturbation of the hydrogen bonding to the bridging oxygen of the Mn−O−M structure, for example, might also account for the observed frequency shift (*42*, *43*). However, because the mid-frequency S_2/S_1 spectrum of D1-D170H PSII particles closely resembles the wild-type* spectrum, even in the amide I region, the frequency shift of the 606 cm^{-1} mode in the D1-D170H spectrum is very unlikely to arise from secondary, nonspecific conformational changes caused by this mutation. Based on the above arguments, we conclude that D1-Asp170 either directly ligates Mn or Ca^{2+} or participates in a hydrogen bond to the Mn_4Ca^{2+} cluster.

In this study, we have demonstrated the great advantage of combining both mid-frequency and low-frequency FTIR techniques with site-directed mutagenesis to explore the structure and coordination environments of the OEC in PSII. We are in the process of adding isotopic labeling to this integrated approach to study structural changes in Mn and Ca^{2+} coordination environments in the different S states of the OEC as part of a strategy to determine the structural mechanism of photosynthetic water oxidation.

REFERENCES

1. Britt, R. D., Peloquin, J. M., and Campbell, K. A. (2000) *Annu. Rev. Biophys. Biomol. Struct. 29*, 463−495.
2. Debus, R. J. (2000) *Met. Ions Biol. Syst. 37*, 657−710.
3. Hoganson, C. W., and Babcock, G. T. (2000) *Met. Ions Biol. Syst. 37*, 613−656.
4. Yocum, C. F., and Pecoraro, V. L. (1999) *Curr. Opin. Chem. Biol. 3*, 182−187.
5. Yachandra, V. K., Sauer, K., and Klein, M. P. (1996) *Chem. Rev. 96*, 2927−2950.
6. Joliot, P., Barbieri, G., and Chabaud, R. (1969) *Photochem. Photobiol. 10*, 309−329.
7. Kok, B., Forbush, B., and McGloin, M. (1970) *Photochem. Photobiol. 11*, 457−475.
8. DeRose, V. J., Yachandra, V. K., McDermott, A. E., Britt, R. D., Sauer, K., and Klein, M. P. (1991) *Biochemistry 30*, 1335−1341.
9. Tang, X.-S., Diner, B. A., Larsen, B. S., Gilchrist, M. L., Jr., Lorigan, G. A., and Britt, R. D. (1994) *Proc. Natl. Acad. Sci. U.S.A. 91*, 704−708.
10. Noguchi, T., Inoue, Y., and Tang, X.-S. (1999) *Biochemistry 38*, 10187−10195.
11. Debus, R. J. (2001) *Biochim. Biophys. Acta 1503*, 164−186.
12. Diner, B. A. (2001) *Biochim. Biophys. Acta 1503*, 147−163.
13. Noguchi, T., Ono, T., and Inoue, Y. (1995) *Biochim. Biophys. Acta 1228*, 189−200.
14. Noguchi, T., Ono, T., and Inoue, Y. (1995) *Biochim. Biophys. Acta 1232*, 59−66.
15. Chu, H.-A., Gardner, M. T., O'Brien, J. P., and Babcock, G. T. (1999) *Biochemistry 38*, 4533−4541.
16. Chu, H.-A., Gardner, M. T., Hillier, W., and Babcock, G. T. (2000) *Photosynth. Res*. (in press).
17. Chu, H.-A., Hillier, W., Law, N. A., and Babcock, G. T. (2001) *Biochim. Biophys. Acta 1503*, 69−82.
18. Chu, H.-A., Sackett, H., and Babcock, G. T. (2000) *Biochemistry 39*, 14371−14376.
19. Diner, B. A., and Nixon, P. J. (1992) *Biochim. Biophys. Acta 1101*, 134−138.
20. Nixon, P. J., and Diner, B. A. (1992) *Biochemistry 31*, 942−948.
21. Boerner, R. J., Nguyen, A. P., Barry, B. A., and Debus, R. J. (1992) *Biochemistry 31*, 6660−6672.
22. Chu, H. A., Nguyen, A. P., and Debus, R. J. (1994) *Biochemistry 33*, 6137−6149.
23. Whitelegge, J. P., Koo, D., Diner, B. A., Domian, I., and Erickson, J. M. (1995) *J. Biol. Chem. 270*, 225−235.
24. Chu, H.-A., Nguyen, A. P., and Debus, R. J. (1995) *Biochemistry 34*, 5839−5858.
25. Campbell, K. A., Force, D. A., Nixon, P. J., Dole, F., Diner, B. A., and Britt, R. D. (2000) *J. Am. Chem. Soc. 122*, 3754−3761.
26. Debus, R. J., Nguyen, A. P., and Conway, A. B. (1990) in *Current Research in Photosynthesis* (Baltscheffsky, M., Ed.) Vol. I, pp 829−832, Kluwer Academic Publishers, Dordrecht, The Netherlands.
27. Debus, R. J., Campbell, K. A., Gregor, W., Li, Z.-L., Burnap, R. L., and Britt, R. D. (2001) *Biochemistry* (in press).
28. Rippka, R., Deruelles, J., Waterbury, J. B., Herdman, M., and Stanier, R. Y. (1979) *J. Gen. Microbiol. 111*, 1−61.
29. Hays, A.-M. A., Vassiliev, I. R., Golbeck, J. H., and Debus, R. J. (1998) *Biochemistry 37*, 11352−11365.
30. Tang, X.-S., and Diner, B. A. (1994) *Biochemistry 33*, 4594−4603.
31. Mishra, R. K., and Ghanotakis, D. F. (1994) *Photosynth. Res. 42*, 37−42.
32. Reifler, M. J., Chisholm, D. A., Wang, J., Diner, B. A., and Brudvig, G. W. (1998) in *Photosynthesis, Mechanisms and effects* (Garab, G., Ed.) Vol. 2, pp 1189−1192, Kluwer Academic Publishers, Dordecht, The Netherlands.
33. Bricker, T. M., Morvant, J., Sutton, H. M., and Frankel, L. K. (1998) *Biochim. Biophys. Acta 1409*, 50−57.
34. Noguchi, T., Inoue, Y., and Tang X.-S. (1997) *Biochemistry 36*, 14705−14711.
35. Noguchi, T., and Sugiura, M. (2000) *Biochemistry 39*, 10943−10949.
36. McDermott, A. E., Yachandra, V. K., Guiles, R. D., Cole, J. L., Dexheimer, S. L., Britt, R. D., Sauer, K., and Klein, M. P. (1988) *Biochemistry 27*, 4021−4031.
37. Aasa, R., Andréasson, L.-E., Lagenfelt, G., and Vänngård, T. (1987) *FEBS Lett. 221*, 245−248.
38. Steenhuis, J. J., Hutchison, R. S., and Barry, B. A. (1999) *J. Biol. Chem. 274*, 14609−14616.
39. Noguchi, T., Ono, T.-A., and Inoue, Y. (1992) *Biochemistry 31*, 5953−5956.
40. Zhang, H. M., Fischer, G., and Wydrzynski, T. (1998) *Biochemistry 37*, 5511−5517.
41. Onoda, K., Mino, H., Inoue, Y., and Noguchi, T. (2000) *Photosynth. Res. 63*, 47−57.
42. Shiemke, A. K., Loehr, T. M., and Sanders-Loehr, J. (1986) *J. Am. Chem. Soc. 108*, 2437−2443.
43. Hanson, M. A., Schmidt, P. P., Strand, K. R., Gräslund, A., Solomon, E. I., and Andersson, K. K. (1999) *J. Am. Chem. Soc. 121*, 6755−6756.

BI0022994